

Research Article

CMaf-Inducing Protein Promotes LUAD Proliferation and Metastasis by Activating the MAPK/ERK Pathway

Xiao-Yan Yu,¹ Ming Wang,² and Juan-Juan Qian ¹

¹Respiratory Medicine, The Second Affiliated Hospital of Jiaxing University, Jiaxing, Zhejiang 314099, China

²Cardiothoracic Surgery, Shulan (Hangzhou) Hospital, Hangzhou, Zhejiang 310015, China

Correspondence should be addressed to Juan-Juan Qian; yymcabc@126.com

Received 27 July 2022; Revised 19 August 2022; Accepted 25 August 2022; Published 14 September 2022

Academic Editor: Xueliang Wu

Copyright © 2022 Xiao-yan Yu et al. This is an open access article distributed under the Creative Commons Attribution License, which permits unrestricted use, distribution, and reproduction in any medium, provided the original work is properly cited.

Objective. Previous studies have shown that cMaf-inducing protein (CMIP) promotes tumorigenesis and progression, however, the role of CMIP in lung adenocarcinoma (LUAD) and its molecular mechanism remain unclear. **Methods.** In this study, the Human Protein Atlas and Kaplan–Meier Plotter database were used to analyze the expression and prognostic value of CMIP in LUAD. Then, the expression levels of CMIP in LUAD tissues and cells were detected by qRT-PCR and western blot. The lentiviral vector was used to establish a stable transfected cell line, and the transfection efficiency was detected by qRT-PCR. MTT assay, colony formation assay, transwell assay, and wound healing assay were used to evaluate the function of CMIP in LUAD. In addition, the effect of CMIP on the MAPK/ERK pathway in LUAD cells was analyzed by western blot. **Results.** The expression level of CMIP was significantly increased in LUAD cell and tissue samples, and the high expression of CMIP was associated with overall survival (OS) and progression-free survival (PFS) in LUAD patients. In vitro experiments showed that CMIP overexpression significantly promoted the proliferation, migration, and invasion of A549 cells. CMIP knockout significantly inhibited the proliferation, migration, and invasion of H1299 cells. In addition, it was observed that the expression levels of the MAPK/ERK pathway-related proteins were significantly increased in CMIP-overexpressed A549 cells, and promoted cell proliferation, migration, and invasion, while U0126 could significantly reverse the activation of the MAPK/ERK pathway by CMIP overexpression, and inhibit the proliferation, migration, and invasion of A549 cells. **Conclusion.** Our study shows that CMIP, as an oncogene, is associated with poor patient prognosis, and may promote the proliferation and metastasis of LUAD by activating the MAPK/ERK pathway. Therefore, CMIP may be a new potential therapeutic target for LUAD.

1. Introduction

According to the latest data from GLOBOCAN in 2020, lung cancer is still the malignant tumor with the highest number of cancer-related deaths in the world, and its mortality rate accounts for about 18.0% of cancer-related deaths [1]. Nonsmall cell lung cancer (NSCLC) accounts for approximately 90% of all lung cancer types, of which adenocarcinoma (LUAD) and squamous cell carcinoma (LUSC) are the most common subtypes [2–4]. At present, radical resection, radiotherapy, and chemotherapy are the traditional methods for clinical treatment of LUAD [5, 6], but the treatment and prognosis of LUAD are poor due to the lack of precise targeting and large side effects and other adverse factors [7].

In addition, due to the high probability of postoperative recurrence and early development of metastatic propensity in LUAD patients [8], the 5-year survival rate of lung cancer patients is only 17% [9], and the 5-year relative survival rate among metastatic patients is only 5% lower [10]. Although many genes involved in LUAD tumorigenesis have been identified at this stage, only a few of them have been developed for clinical treatment. Therefore, finding potential cancer-related genes and elucidating their biological mechanisms related to tumor malignant behavior has important therapeutic significance.

CMaf-inducing protein (CMIP) was originally discovered in the podocytes of patients with acquired idiopathic nephrotic syndrome [11]. The protein structure of CMIP

consists of an N-terminal region of the pleckstrin homology domain (PH), an intermediate region containing multiple interacting docking sites (a 14-3-3 module, a PKC domain, and an SH3 domain similar to the p85, the regulatory subunit of phosphatidylinositol 3-kinase (PI3K)) and a C-terminal region containing a leucine-rich repeat (LRR) domain [12]. At present, the function of CMIP is still unclear. Previous studies have shown that intravenous injection of small interfering RNA-targeting CMIP can prevent lipopolysaccharide-induced proteinuria in rats by inhibiting the interaction between Src kinase Fyn and cytoskeletal regulator N-WASP (neural Wiskott Aldrich syndrome protein) and between adaptor proteins Nck and nephrin [11]. CMIP interacts with RelA to inhibit the degradation of I- κ B α and prevent the dissociation of the NF- κ B/I- κ B α complex, resulting in down-regulation of NF- κ B activity [13]. In addition, Kamal et al. found that CMIP has a dual effect in undifferentiated T cells, when CMIP inactivates Lck by interacting with the p85 subunit of PI3 kinase, leading to activation of the extracellular signal-regulated kinase (ERK) 1/2 and P38 MAPK pathways, but when CMIP interacts with death-associated protein kinase (DAPK)-interacting protein-1 (DIP-1) and upregulates DAPK, it blocks the nuclear translocation of ERK1/2 and thus plays a key role in preventing the development of immune responses [14]. Studies have found that two isoforms of adaptor proteins of CMIP are expressed in the human brain [15, 16] and play an important role in human reading [16] and language [17]-related behavioral traits by participating in the cMaf signaling pathway. To date, little is known about CMIP in cancer. Zhang et al. showed that high expression of CMIP in gastric cancer tissue is associated with poorer clinical parameters, RFS, and OS, and CMIP works by upregulating mitogen-activated protein kinase (MAPK). Its expression plays an oncogenic role in human gastric cancer cells [18]. However, the relationship and mechanism of action of CMIP in LUAD have not been reported.

In the present study, CMIP protein expression was significantly elevated in LUAD tissue compared with normal lung tissue and correlated with poorer overall survival (OS) and progression-free survival (PFS). In addition, CMIP overexpression promoted the proliferation, migration, and invasion of lung cancer cells. Notably, CMIP overexpression activated the MAPK/ERK signaling pathways to promote LUAD development, while U0126 reversed the oncogenic effects of CMIP. It indicated that CMIP may promote the proliferation and metastasis of LUAD by activating the MAPK/ERK pathway. CMIP can be further studied as a prognostic biomarker and clinical therapeutic target for LUAD.

2. Materials and Methods

2.1. Clinical Samples. We collected a total of 20 tumor tissue samples (LUAD) and paired adjacent normal tissue (Normal) from patients diagnosed with LUAD between June 2018 and December 2020. All patients were admitted to Shulan (Hangzhou) Hospital, and all participants signed informed consent voluntarily. In this study, two pathologists

diagnosed LUAD based on the pathological results, and analyzed the histological type and tumor stage of the patients according to the eighth edition of the Lung Cancer Tumor, Lymph Node, Metastasis (TNM) Staging System [19]. This study was approved by the Research Ethics Committee of Shulan (Hangzhou) Hospital (KY2022042). The study was conducted in accordance with the Declaration of Helsinki (revised 2013).

The inclusion criteria are as follows [20]: (1) Have not received chemotherapy and radiotherapy; (2) No history of any other malignant tumor within 5 years; (3) No pregnancy or breastfeeding; (4) No cardiopulmonary insufficiency and severe cardiovascular disease; (5) No severe infection and severe malnutrition.

2.2. Data Collection. The human protein atlas (HPA; <https://www.proteinatlas.org>), immunohistochemical (IHC) staining data of CMIP in normal lung tissues, and LUAD tissues were obtained. In the HPA database, protein expression was scored on four levels of undetected, low, medium, and high based on the proportion of stained cells and the intensity of staining [21].

The Kaplan–Meier Plotter database (<http://www.kmplot.com>) was used for survival analysis of CMIP mRNA expression in LUAD patients, including OS and PFS, to evaluate LUAD patients prognosis. The LUAD patients were divided into high-expression group and low-expression group according to the median expression value, and the “Automatically select the best cutoff” model was selected during the analysis and the threshold with the best performance was used as the cutoff value. Results are shown graphically with hazard ratios (HR) and log-rank test *P* values with 95% confidence intervals, and log-rank test *P* values of $p < 0.05$ were considered statistically significant [22].

2.3. Cell Culture and Transfection. Cell culture human normal lung epithelial cells (BEAS-2B) and human nonsmall cell lung cancer cell lines (A549, H460 and H1299) were purchased from American type culture collection (ATCC). The cells were cultured in DMEM or RPMI-1640 medium (GIBCO, USA) supplemented with 10% fetal bovine serum (FBS; GIBCO, USA) and 100 U/ml of penicillin streptomycin mixed antibiotics, and the cells were cultured in a humidified incubator at 37°C and 5% CO₂.

Cell transfection CMIP siRNA plasmid (si-CMIP) and negative siRNA plasmid (siNC), empty plasmid pcDNA3.1 (Vector), and CMIP overexpression plasmid pcDNA3.1-CMIP (OE-CMIP) were designed and synthesized by Thermo Fisher Scientific. H460 and H1299 cells (1×10^6 cells/mL) were seeded in 6-well plates, grouped, and transfected when the cells grew to 80%–90%. Transfected H460 cells grouped: vector group and OE-CMIP group. Transfected H1299 cells grouped: siNC group and si-CMIP group. The plasmids were transfected into H460 and H1299 cells, respectively, using Lipofectamine™ 2000 transfection reagent (11668500, Invitrogen, Thermo Fisher Scientific, Inc.) according to the manufacturer’s instructions. After 6 h

TABLE 1: Primers.

Gene	Sequences (5' to 3')
CMIP	F: AAATTCCTGAGGCGCTG R: CTTCAATTGCGCTGTAGGA
β -actin	F: TTCCTGGGCATGGAGTC R: CAGGTCTTTGCGGATGTC

of transfection, the medium was changed and the cells were cultured for another 48 h. Cells are collected. Transfection efficiency was detected using qRT-PCR.

2.4. Quantitative Real-Time PCR Analysis (qRT-PCR). Total RNA from cells and tissues was extracted using the TRIzol™ Plus RNA Purification Kit (Invitrogen, Thermo Fisher Scientific, Inc.) according to the manufacturer's instructions, and RNA was reverse transcribed into cDNA according to the instructions of PrimeScript RTMaster Mix (Takara, Japan). Also, the concentration and purity of cDNA were checked. qRT-PCR was performed using the SYBR PremixEx Taq II kit (Takara, Japan) to detect the relative expression levels of CMIP. PCR amplification steps: 95°C for 30 s; 95°C for 5 s, 60°C for 30 s, 72°C for 45 s, 40 cycles; 72°C for 10 min. β -actin was used as an internal reference gene and the data were analyzed by the $2^{-\Delta\Delta Ct}$ method [23]. The primer sequences are shown in Table 1.

2.5. Cell Viability Assays. Transfected H1299 and H460 cells were seeded in 96-well plates at 5×10^3 cells/well. H460 cells were treated with or without the addition of 10 μ M U0126 [24–26] (#9903S, Cell Signal Technology, Danvers, MA, USA). After 24 h of cell culture, 10 μ L of MTT (5 mg/ml) (Biyuntian, China) was added to each well, and then incubated at 37°C for 4 h. The supernatant was aspirated and 150 μ L of DMSO was added to each well. The absorbance of each well was measured at 570 nm using a microplate reader (Bio-Rad Laboratory, Inc.) [27]. All experiments were repeated three times.

2.6. Cell Colony Formation Assay. Transfected H1299 cells and H460 cells were seeded into 6-well plates at 500 cells/well, and H460 cells were treated with or without the addition of 10 μ M U0126. The new medium was replaced every 3 days, and after 2 weeks of culture, cells were fixed with 4% paraformaldehyde for 30 min at room temperature and stained with 0.1% crystal violet for 30 min. Photographs were taken using a light microscope (Olympus Corporation, Japan) and the number of visible colonies were manually counted. Groups of cells containing >50 cells were identified as colonies, and the number of clones in each group was counted [28]. All experiments were repeated three times.

2.7. Wound Healing Assay. Transfected H1299 cells and H460 cells were seeded into 6-well plates at 5×10^4 cells/well, and H460 cells were treated with or without the addition of 10 μ M U0126. When the cells reached 90% confluency, a 20 μ L pipette tip was used to scratch directly on the cell

monolayer and wash the cells with PBS. They were then incubated in serum-free RPMI-1640 for 24 h. Images were taken at 0 h and 24 h using a light microscope (Leica, Germany), and ImageJ software was used to quantitatively assess the wound area and calculate cell migration rates for each group [28]. All experiments were repeated three times.

2.8. Transwell Assay. Matrigel (364262, BD Biosciences) was coated on a 24-well transwell chamber (Costar; Corning, Inc.) at 37°C and placed in a cell incubator overnight. After suspending transfected H1299 cells and H460 cells with FBS-free medium, 100 μ L of cells were seeded into the upper chamber at 5×10^5 cells/ml, and 500 μ L of RPMI-1640 containing 10% FBS was added to the lower chamber. H460 cells were treated with or without the addition of 10 μ M U0126. After culturing at 37°C for 24 h, cells on the underside of the membrane were fixed with 5% glutaraldehyde for 30 min at 4°C, and then stained with 0.5% crystal violet for 30 min at room temperature. Images were taken using an inverted light microscope (Leica, Germany) and invading cells in different areas were counted and analyzed using ImageJ software [29]. All experiments were repeated three times.

2.9. Western Blot Analysis. Transfected H1299 cells and H460 cells were seeded into 6-well plates at 1×10^6 cells/well, and the cells were collected when the cells reached a certain number. Total cell and tissue proteins were extracted using RIPA lysis buffer (Beyotime, Shanghai, China) containing protease and phosphatase inhibitors. Protein concentrations were determined using the BCA protein assay kit (Beyotime). Equal amounts of protein samples (30 μ g/lane) were separated on 8–12% SDS–polyacrylamide gel electrophoresis (PAGE), and proteins were transferred to polyvinylidene fluoride membranes (PVDF, Immobilon-P, Millipore). Afterward, membranes were blocked with 5% skim milk or bovine serum albumin (BSA) (for phosphorylated proteins) for 1 h at room temperature. Then at 4°C with primary antibodies CMIP (PA5-65870, Invitrogen); P38 (#9212, Cell Signaling Technology); ERK (#4695, Cell Signaling Technology); p-P38 (#9215, Cell Signaling Technology); p-ERK (#4370, Cell Signaling Technology) and β -actin (#3700, Cell Signaling Technology) were incubated overnight. After TBST washes, the membranes were incubated with the appropriate horseradish peroxidase-conjugated secondary antibodies goat anti-rabbit IgG H&L (HRP) (ab205718, Abcam) and goat anti-mouse IgG H&L (HRP) (ab97023, Abcam) was incubated for 2 h. Images of protein bands were obtained using ECL chemiluminescent liquid (PE0010, Solebao). The target protein expression levels were calculated and normalized using Image J software.

2.10. Statistical Analysis. All experiments were repeated at least three times and all statistical analyses were analyzed using SPSS 26.0 software or GraphPad Prism 8.0. All data are presented as mean \pm SD. Differences between multiple groups were analyzed using one-way ANOVA and

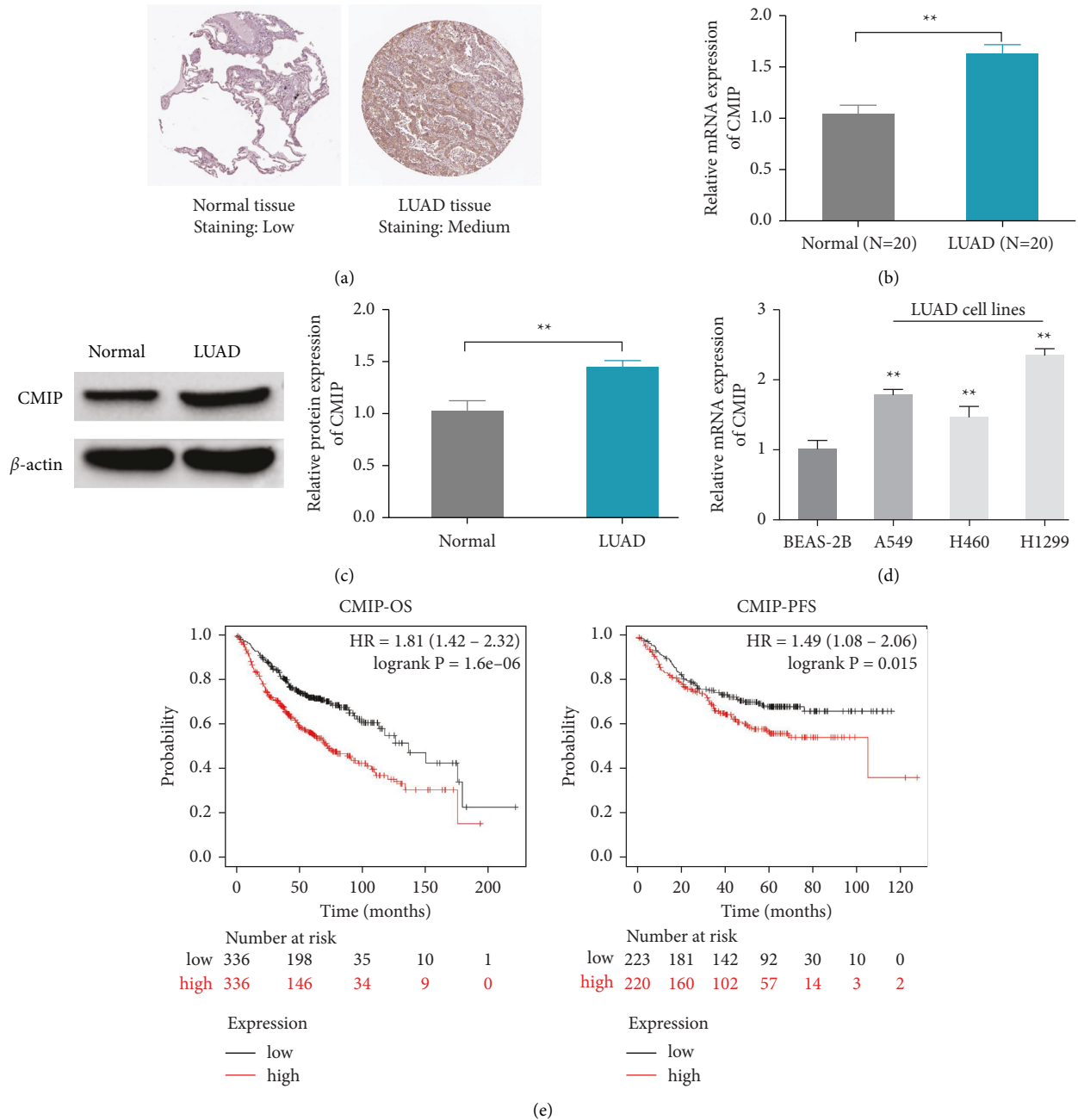


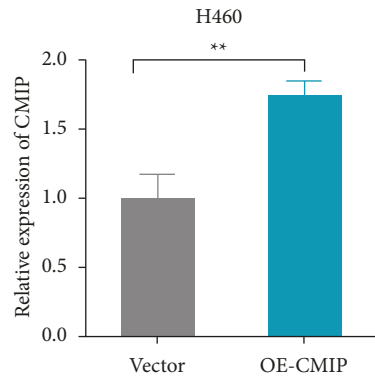
FIGURE 1: CMIP is upregulated in LUAD and associated with poor prognosis. (a) Immunohistochemical tissue microarray image (HPA) of CMIP protein. (b) qRT-PCR detection of CMIP mRNA levels in normal lung tissue and LUAD tissue ($n = 20$); (c) Western blot detection of CMIP protein expression in normal lung tissue and LUAD tissue ($n = 3$); (d) mRNA levels of CMIP detected by qRT-PCR in BEAS-2B, A549, H460, and H1299 cells ($n = 3$); (e) OS and PFS in LUAD patients obtained from the Kaplan-Meier plotter online database; ** $P < 0.01$ vs. (Normal group or BEAS-2B group).

Bonferroni's multiple comparison post hoc test. $P < 0.05$ was considered to be statistically significant.

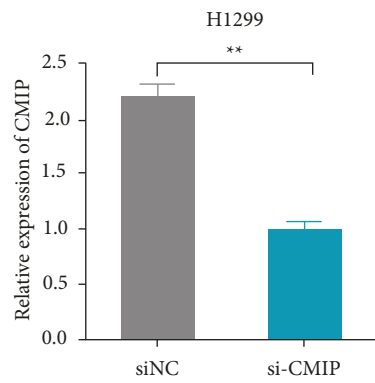
3. Results

3.1. CMIP Is Upregulated in LUAD and Associated with Poor Prognosis. To determine the relationship between CMIP expression and LUAD, tissue microarray IHC according to the HPA database showed that the expression of CMIP was

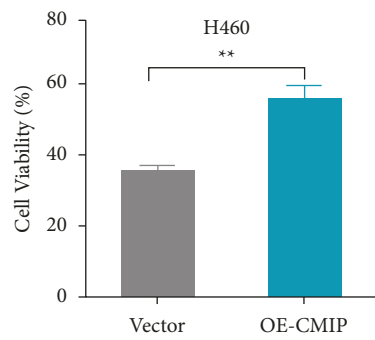
significantly higher in LUAD tissue than in normal lung tissue (Figure 1(a)). Similarly, CMIP protein levels were significantly elevated in LUAD tissues and cells were confirmed by qRT-PCR and Western blot analysis. It is worth noting that among the three lung cancer cell lines, CMIP expression was highest in H1299 cells and lowest in H460 cells (Figures 1(b)–e), therefore, knockdown of CMIP in H1299 cells and overexpression of CMIP in H460 cells were selected for subsequent experimental studies.



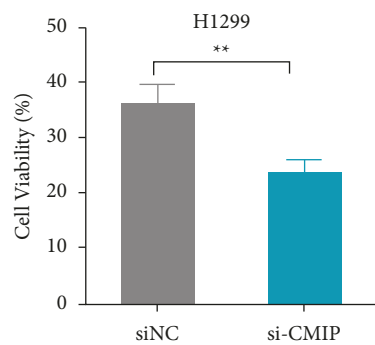
(a)



(b)



(c)



(d)

FIGURE 2: Continued.

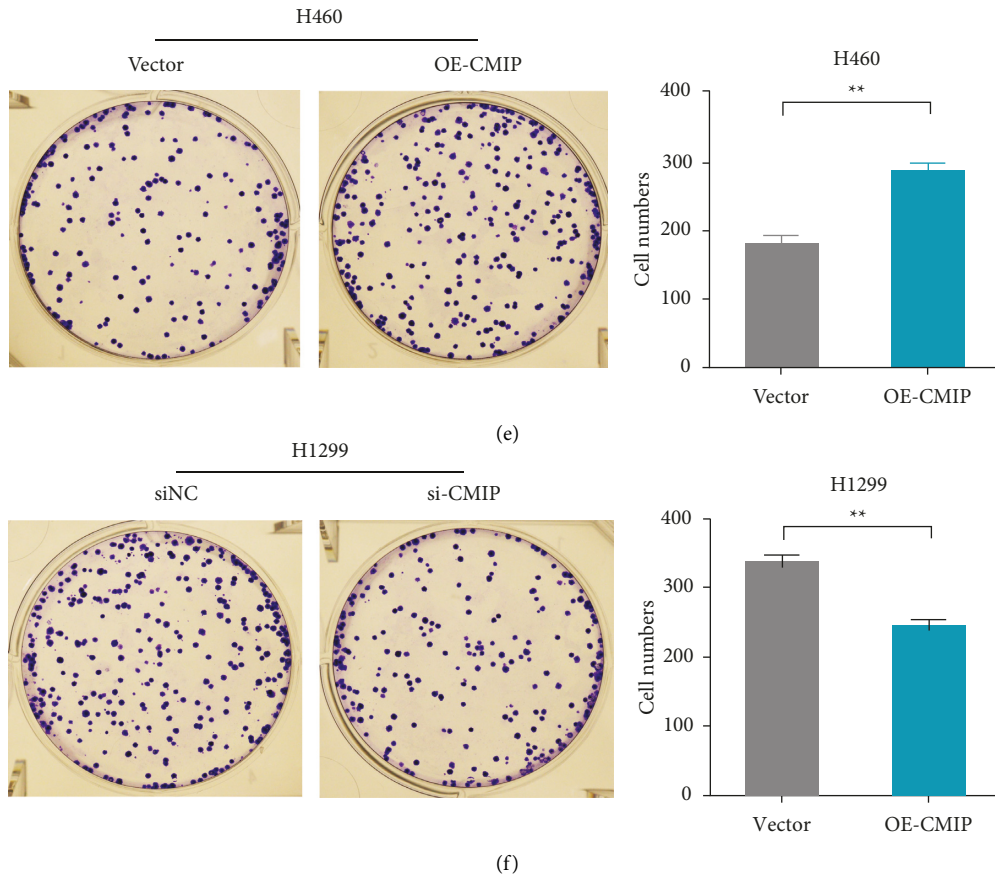


FIGURE 2: CMIP overexpression promotes the proliferation of H460 cells. (a/b) The mRNA levels of CMIP in H460 (a) and H1299 (b) cells after transfection were detected by qRT-PCR; (c/d) MTT assay was used to detect the difference of CMIP expression after transfection on H460 (c) and H1299 (d) Effect of cell viability. (e/f) Cell colony formation assay to assess the effect of CMIP expression on the proliferation of H460 (e) and H1299 (f) cells after transfection. ** $P < 0.01$ vs. (siNC group or vector group).

Furthermore, using Kaplan–Meier survival curves, it was found that patients with high CMIP expression in LUAD had worse OS ($P = 0.0068$) and PFS ($P = 0.015$) (Figure 1(f)). Therefore, these results suggest that CMIP is involved in the occurrence and development of LUAD, which is worthy of further study.

3.2. CMIP Overexpression Promotes H460 Cell Proliferation.

In order to explore the effect of CMIP on the occurrence and development of LUAD, this study firstly transfected CMIP overexpression or knockdown plasmids into H460 and H1299 cells, respectively. qRT-PCR detection showed that in H460 cells, compared with the vector group, CMIP mRNA level in the OE-CMIP group was significantly increased (Figure 2(a)). In H1299 cells, CMIP mRNA levels were significantly decreased in the si-CMIP group compared with the siNC group (Figure 2(b)). Subsequently, the effect of CMIP expression on the viability of H460 and H1299 cells was examined by MTT. The results showed that CMIP overexpression significantly enhanced H460 cell viability compared with the vector group (Figure 2(c)), while in H1299 cells, knockdown of CMIP significantly inhibited cell viability compared with the siNC group (Figure 2(d)). In addition, the

cell colony formation assay showed that CMIP overexpression significantly increased the number of H460 cell colonies compared with the vector group (Figure 2(e)). Compared with the siNC group, knockdown of CMIP significantly reduced the number of H1299 cell colonies (Figure 2(f)).

3.3. CMIP Overexpression Promotes H460 Cell Migration and Invasion.

Subsequently, we further assessed the effect of CMIP expression on the migration and invasion of H460 and H1299 cells. The results showed that CMIP overexpression significantly promoted H460 cell migration and invasion compared with the vector group (Figures 3(a) and 3(c)), and knockdown of CMIP significantly inhibited H1299 cell migration and invasion compared with the siNC group (Figures 3(b) and 3(d)). These results indicate that high expression of CMIP promotes the occurrence and development of LUAD.

3.4. CMIP Overexpression Promotes Activation of MAPK/ERK Signaling Pathway.

In order to explore the molecular mechanism of abnormal expression of CMIP in the

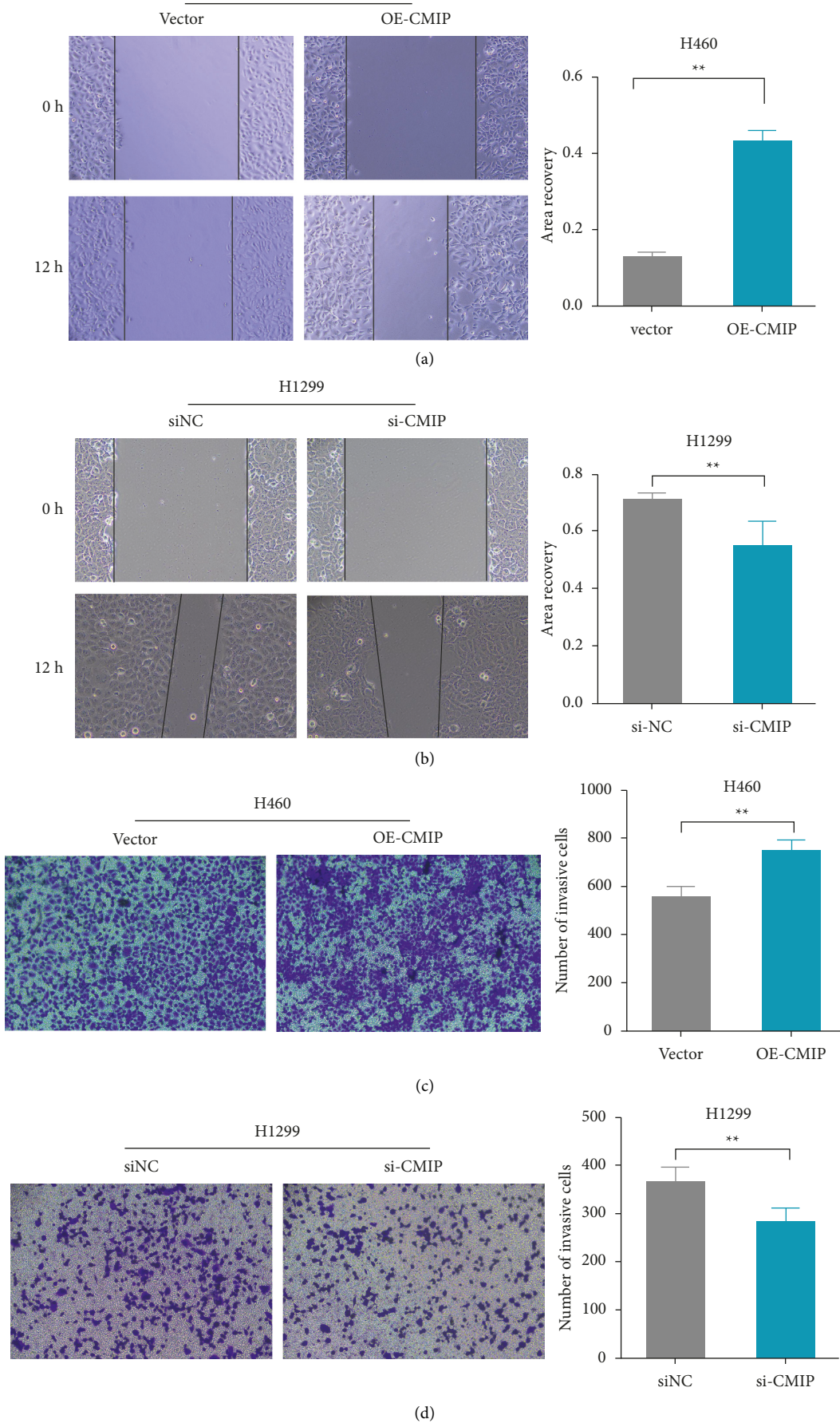


FIGURE 3: CMIP overexpression promotes H460 cell migration and invasion. (a/b) The wound healing assay was used to analyze the effect of CMIP expression on the migration of H460 (a) and H1299 (b) cells after transfection. (c/d) The effect of CMIP expression on H460 (c) and H1299 (d) cell invasion after transfection was assessed using Transwell analysis. ** $P < 0.01$ vs. (siNC group or vector group).

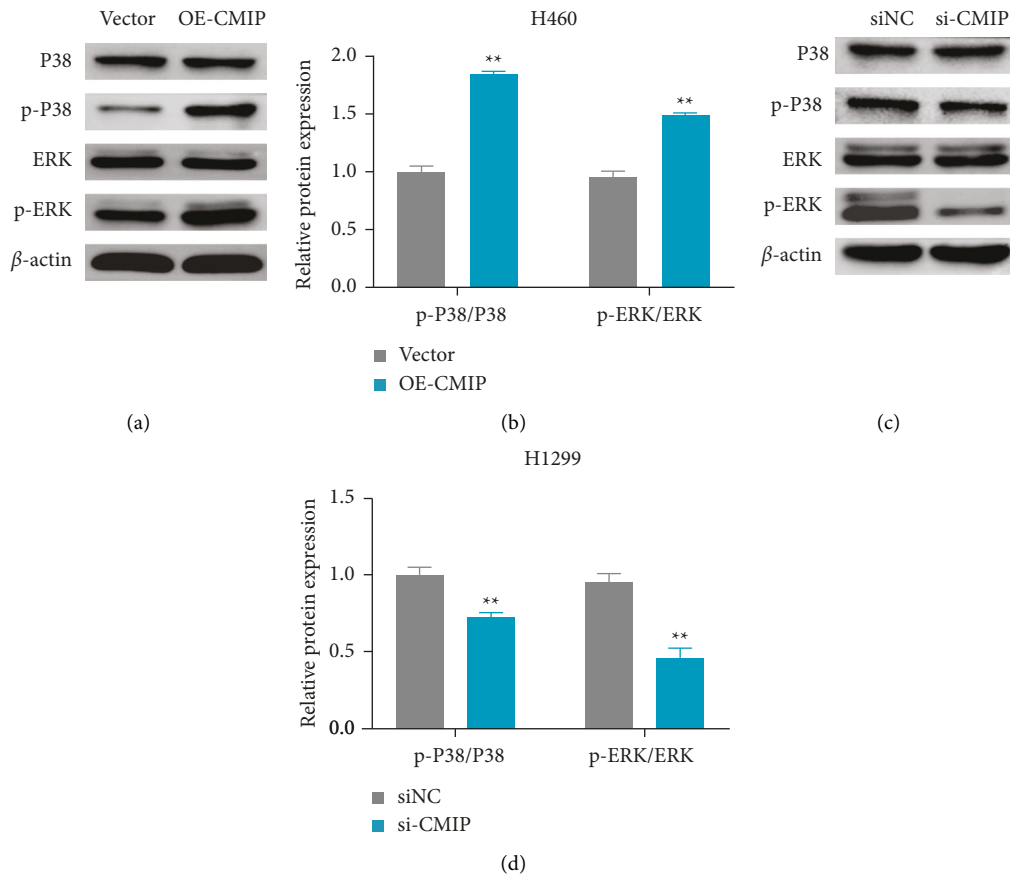


FIGURE 4: CMIP overexpression promotes activation of the MAPK/ERK pathway. (a, b) Western blot detection of P38, ERK, p-P38 and p-ERK protein expression, and the relative expression of p-P38/P38 and p-ERK/ERK in H1299 cells. (c, d) Western blot detection of P38, ERK, p-P38 and p-ERK protein expression, and the relative expression of p-P38/P38 and p-ERK/ERK in H460 cells. ** $P < 0.01$ vs. (siNC group or vector group).

occurrence and development of LUAD, this study detected the expression of the MAPK/ERK pathway-related proteins. Western blot analysis showed that knockdown of CMIP significantly reduced p-P38 and p-ERK protein expressions, and p-P38/P38 and p-ERK/ERK ratios in H1299 cells compared with the siNC group (Figures 4(a) and 4(b)). In H460 cells, CMIP overexpression significantly increased p-P38 and p-ERK protein expression, and p-P38/P38 and p-ERK/ERK ratios compared with the vector group (Figures 4(c) and 4(d)). These results suggest that the MAPK/ERK pathways may be involved in the pathogenesis of LUAD by CMIP.

3.5. CMIP Overexpression Promotes H460 Cell Proliferation, Migration, and Invasion by Activating the MAPK/ERK Pathway. In addition, in order to further verify whether CMIP overexpression promotes the occurrence and development of LUAD through MAPK/ERK, H460 cells were treated with $10 \mu\text{M}$ U0126, and the results of MTT assay showed that compared with the OE-CMIP group, OE-CMIP + U0126 group significantly reduced the number of cells viability (Figure 5(a)). Colony formation assays also showed similar results, with U0126 intervention significantly reducing the number of H460 cell colonies compared to the

OE-CMIP group (Figure 5(b)). In addition, wound healing assay and transwell analysis showed that the migration and invasion of H460 cells were significantly inhibited after U0126 intervention compared with the OE-CMIP group (Figures 5(c) and 5(d)). These results suggest that CMIP overexpression promotes the progression of LUAD by activating the MAPK/ERK pathway.

4. Discussion

At present, lung cancer is still one of the malignant tumors that seriously endanger human health and life [1]. With the rapid development of various omics technologies and bioinformatics, more and more genes have been identified as biomarkers for certain cancers for disease screening, diagnosis, prognosis, or further development as therapeutic targets corresponding biological reagents. Wei et al. found that EHD2 can inhibit the invasive ability of LUAD, improve patient prognosis, and can be used as a prognostic biomarker for LUAD [30]. Huang et al. showed through bioinformatics analysis and cellular experiments that high expression of GRSF1 promotes the occurrence and development of LUAD tumors and can be used as an effective prognostic biomarker for LUAD patients [31]. Previous studies have shown that CMIP, as an oncogene, promotes the progression of human

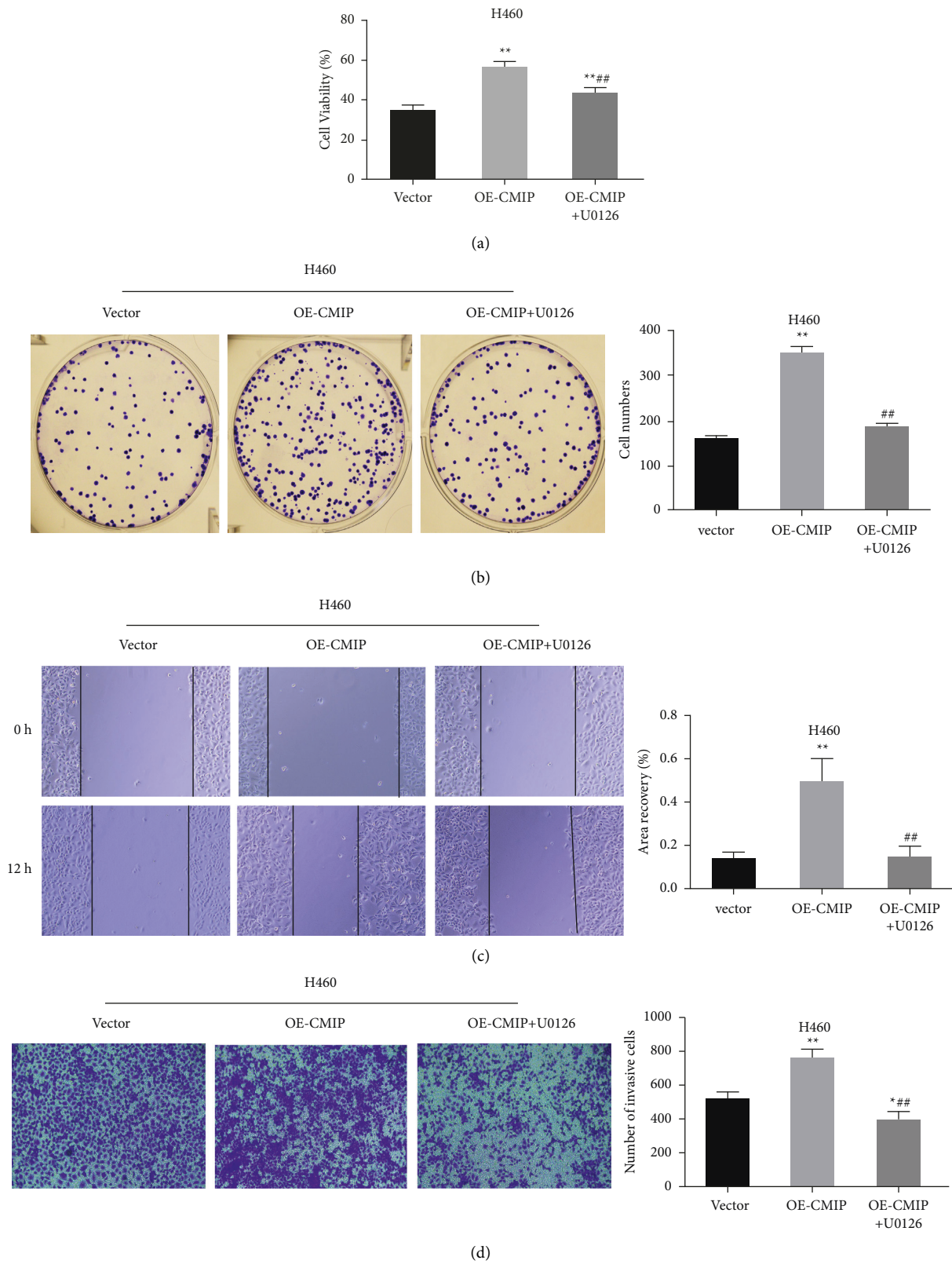


FIGURE 5: CMIP promotes H460 cell proliferation, migration, and invasion by activating the MAPK/ERK pathway. (a) MTT assay to detect cell viability in each group; (b) cell clone formation assay to detect the number of cell clones in each group; (c) wound healing assay to detect cell migration in each group; (d) Transwell analysis to detect cell invasion ability of each group. * $P < 0.05$ and ** $P < 0.01$ vs. vector group, ## $P < 0.01$ vs. OE-CMIP group.

gastric cancer and human glioma, and may be a potential target for the diagnosis and treatment of human glioma [18, 32]. However, so far, no studies have addressed the relationship between CMIP and LUAD. In the present study, bioinformatics analysis found that CMIP was highly expressed in LUAD tissues and correlated with poor patient prognosis. Subsequently, by detecting the expression of CMIP at the mRNA and protein levels, the results showed that the expression of CMIP in LUAD tissues and cells was significantly higher than that in the control group. These findings suggest that CMIP can serve as a prognostic biomarker for LUAD and is a new potential target worth investigating.

In order to explore the role of CMIP in LUAD and its molecular mechanism, this study found that CMIP overexpression promoted the proliferation, migration, and invasion of H460 cells through *in vitro* cell experiments, however, CMIP knockout significantly inhibited the proliferation, migration of H1299 cells, and invasive capacity, these results are consistent with Wang et al. [32]. In contrast, Zhang et al., in addition to demonstrating that CMIP knockout significantly reduced the proliferation, migration, and invasion abilities of MKN-28 gastric cancer cells, also showed that apoptosis was significantly increased after CMIP knockout by flow cytometry [18]. Based on this, the apoptotic role of CMIP in LUAD needs to be addressed in future studies.

Previous studies have shown that CMIP can directly inhibit Src kinase and cause urinary protein in mice [11]. In addition, Src homologous collagen (Shc) protein stimulates Raf through GTPase-Ras to activate the MAPK pathway, especially the ERK pathway to promote cell proliferation [33]. It has been reported that overactivation of the MAPK pathway promotes the occurrence and development of LUAD [34–36]. A previous study reported that EphA10 drives tumor progression and immune evasion by regulating the MAPK/ERK cascade in LUAD, and the MEK inhibitor U0126 significantly reversed the promoting effect of EphA10 overexpression on LUAD cells [37]. In this study, western blot experiments showed that CMIP overexpression significantly increased the expression of MAPK/ERK pathway-related proteins in H460 cells, while U0126 could significantly reversed the function of CMIP overexpression on the activation of the MAPK/ERK pathway. Therefore, CMIP may play pro-proliferation, migration and invasion effects in LUAD by activating the MAPK/ERK pathway.

To our knowledge, this study is the first to report the oncogenic role of CMIP in LUAD. Through bioinformatics analysis, clinical tissue samples and *in vitro* cell experiments, it was proved that high expression of CMIP is associated with poor prognosis of patients, and may promote the development of LUAD by activating the MAPK/ERK pathway. However, this study has some limitations. For the first time, the effect of CMIP on the malignant characteristics of LUAD by activating the MAPK/ERK pathway was not further explored in animal models by breeding CMIP knockout mice or injecting CMIP-targeting small interfering RNAs in LUAD mice. Second, epithelial-mesenchymal transition (EMT) promotes the spread of early epithelial cancer cells and is an important parameter for assessing the

ability of epithelial cancer to metastasize and invade [38, 39] the degree of tumor resistance to anticancer drugs [40–42], but, which we did not explore in this study. Therefore, these issues will be addressed in future studies.

5. Conclusion

In conclusion, CMIP expression was significantly elevated in both LUAD cell lines and tissues, and was significantly associated with poor patient prognosis. Furthermore, CMIP promoted the proliferation and metastasis of LUAD cells by activating the MAPK/ERK pathway. Therefore, CMIP can serve as a prognostic biomarker and potential therapeutic target for LUAD.

Data Availability

The data used to support the findings of this study are available from the corresponding author upon request.

Conflicts of Interest

The authors declare that they have no conflicts of interest.

References

- [1] H. Sung, J. Ferlay, R. L. Siegel et al., “Global cancer statistics 2020: GLOBOCAN estimates of incidence and mortality worldwide for 36 cancers in 185 countries,” *CA: A Cancer Journal for Clinicians*, vol. 71, no. 3, pp. 209–249, 2021.
- [2] J. R. Molina, P. Yang, S. D. Cassivi, S. E. Schild, and A. A. Adjei, “Non-small cell lung cancer: epidemiology, risk factors, treatment, and survivorship,” *Mayo Clinic Proceedings*, vol. 83, no. 5, pp. 584–594, 2008.
- [3] W. D. Travis, E. Brambilla, M. Noguchi et al., “International association for the study of lung cancer/American thoracic society/European respiratory society: international multidisciplinary classification of lung adenocarcinoma: executive summary,” *Proceedings of the American Thoracic Society*, vol. 8, no. 5, pp. 381–385, 2011.
- [4] Z. Chen, C. M. Fillmore, P. S. Hammerman, C. F. Kim, and K. K. Wong, “Non-small-cell lung cancers: a heterogeneous set of diseases,” *Nature Reviews Cancer*, vol. 14, no. 8, pp. 535–546, 2014.
- [5] U. Testa, G. Castelli, and E. Pelosi, “Lung cancers: molecular characterization, clonal heterogeneity and evolution, and cancer stem cells,” *Cancers*, vol. 10, no. 8, p. 248, 2018.
- [6] J. Hanaoka, M. Yoden, K. Hayashi et al., “Dynamic perfusion digital radiography for predicting pulmonary function after lung cancer resection,” *World Journal of Surgical Oncology*, vol. 19, no. 1, p. 43, 2021.
- [7] L. N. R. Buddharaju and A. K. Ganti, “Immunotherapy in lung cancer: the chemotherapy conundrum,” *Chinese Clinical Oncology*, vol. 9, no. 4, p. 59, 2020.
- [8] J. Zhang, J. Fujimoto, J. Zhang et al., “Intratumor heterogeneity in localized lung adenocarcinomas delineated by multi-region sequencing,” *Science (New York, N.Y.)*, vol. 346, no. 6206, pp. 256–259, 2014.
- [9] Y. Zhao, F. Varn, G. Cai, F. Xiao, C. Amos, and C. Cheng, “A P53-deficiency gene signature predicts recurrence risk of patients with early-stage lung adenocarcinoma,” *Cancer Epidemiology, Biomarkers & Prevention*, vol. 27, no. 1, pp. 86–95, 2018.

- [10] R. L. Siegel, K. D. Miller, and A. Jemal, "Cancer statistics, 2020," *CA: A Cancer Journal for Clinicians*, vol. 70, no. 1, pp. 7–30, 2020.
- [11] S. y. Zhang, M. Kamal, K. Dahan et al., "c-mip impairs podocyte proximal signaling and induces heavy proteinuria," *Science Signaling*, vol. 3, no. 122, p. ra39, 2010.
- [12] D. Sahali, K. Sendeyo, M. Mangier et al., "Immunopathogenesis of idiopathic nephrotic syndrome with relapse," *Seminars in Immunopathology*, vol. 36, no. 4, pp. 421–429, 2014.
- [13] M. Kamal, A. Valanciute, K. Dahan et al., "C-mip interacts physically with RelA and inhibits nuclear factor kappa B activity," *Molecular Immunology*, vol. 46, no. 5, pp. 991–998, 2009.
- [14] M. Kamal, A. Pawlak, F. BenMohamed et al., "C-mip interacts with the p85 subunit of PI3 kinase and exerts a dual effect on ERK signaling via the recruitment of Dip1 and DAP kinase," *FEBS Letters*, vol. 584, no. 3, pp. 500–506, 2010.
- [15] K. Szymańska, K. Szczałuba, A. Lugowska et al., "The analysis of genetic aberrations in children with inherited neuro-metabolic and neurodevelopmental disorders," *BioMed Research International*, vol. 2014, pp. 1–8, 2014.
- [16] D. F. Newbury, L. Winchester, L. Addis et al., "CMIP and ATP2C2 modulate phonological short-term memory in language impairment," *The American Journal of Human Genetics*, vol. 85, no. 2, pp. 264–272, 2009.
- [17] T. S. Scerri, A. P. Morris, L. L. Buckingham et al., "DCDC2, KIAA0319 and CMIP are associated with reading-related traits," *Biological Psychiatry*, vol. 70, no. 3, pp. 237–245, 2011.
- [18] J. Zhang, J. Huang, X. Wang et al., "CMIP is oncogenic in human gastric cancer cells," *Molecular Medicine Reports*, vol. 16, no. 5, pp. 7277–7286, 2017.
- [19] R. Rami-Porta, V. Bolejack, J. Crowley et al., "The IASLC lung cancer staging project: proposals for the revisions of the T descriptors in the forthcoming eighth edition of the TNM classification for lung cancer," *Journal of Thoracic Oncology*, vol. 10, no. 7, pp. 990–1003, 2015.
- [20] L. Wang, L. Meng, X. w. Wang, G. y. Ma, and J. h. Chen, "Expression of RRM1 and RRM2 as a novel prognostic marker in advanced non-small cell lung cancer receiving chemotherapy," *Tumor Biology*, vol. 35, no. 3, pp. 1899–1906, 2014.
- [21] A. Digre and C. Lindskog, "The Human Protein Atlas-Spatial localization of the human proteome in health and disease," *Protein Science*, vol. 30, no. 1, pp. 218–233, 2021.
- [22] A. Lánckzy and B. Györffy, "Web-based survival analysis tool tailored for medical Research (KMplot): development and implementation," *Journal of Medical Internet Research*, vol. 23, no. 7, Article ID e27633, 2021.
- [23] K. J. Livak and T. D. Schmittgen, "Analysis of relative gene expression data using real-time quantitative PCR and the 2- $\Delta\Delta$ CT method," *Methods*, vol. 25, no. 4, pp. 402–408, 2001.
- [24] M. Y. Li, Y. Liu, L. Z. Liu et al., "Estrogen receptor alpha promotes smoking-carcinogen-induced lung carcinogenesis via cytochrome P450 1B1," *Journal of Molecular Medicine (Berlin)*, vol. 93, no. 11, pp. 1221–1233, 2015.
- [25] J. H. Joo, G. Liao, J. B. Collins, S. F. Grissom, and A. M. Jetten, "Farnesol-induced apoptosis in human lung carcinoma cells is coupled to the endoplasmic reticulum stress response," *Cancer Research*, vol. 67, no. 16, pp. 7929–7936, 2007.
- [26] M. L. Janmaat, J. A. Rodriguez, M. Gallegos-Ruiz, F. A. Kruyt, and G. Giaccone, "Enhanced cytotoxicity induced by gefitinib and specific inhibitors of the Ras or phosphatidylinositol-3 kinase pathways in non-small cell lung cancer cells," *International Journal of Cancer*, vol. 118, no. 1, pp. 209–214, 2006.
- [27] P. Twentyman and M. Luscombe, "A study of some variables in a tetrazolium dye (MTT) based assay for cell growth and chemosensitivity," *British Journal of Cancer*, vol. 56, no. 3, pp. 279–285, 1987.
- [28] L. Dai, S. Li, X. Li, and B. Jiang, "Propofol inhibits the malignant development of osteosarcoma U2OS cells via AMPK/FOXO1-mediated autophagy," *Oncology Letters*, vol. 24, no. 3, p. 310, 2022.
- [29] S. J. Wang, W. W. Li, C. J. Wen, Y. L. Diao, and T. L. Zhao, "MicroRNA-214 promotes the EMT process in melanoma by downregulating CADM1 expression," *Molecular Medicine Reports*, vol. 22, no. 5, pp. 3795–3803, 2020.
- [30] S. Wei, J. Shao, J. Wang et al., "EHD2 inhibits the invasive ability of lung adenocarcinoma and improves the prognosis of patients," *Journal of Thoracic Disease*, vol. 14, no. 7, pp. 2652–2664, 2022.
- [31] R. Huang, L. Xu, Q. Chen et al., "GRSF1 predicts an unfavorable prognosis and promotes tumorigenesis in lung adenocarcinoma based on bioinformatics analysis and *in vitro* validation," *Annals of Translational Medicine*, vol. 10, no. 13, p. 747, 2022.
- [32] B. Wang, Z. s. Wu, and Q. Wu, "CMIP promotes proliferation and metastasis in human glioma," *BioMed Research International*, vol. 2017, pp. 1–8, 2017.
- [33] A. Józefiak, M. Larska, M. Pomorska-Mól, and J. J. Ruszkowski, "The IGF-1 signaling pathway in viral infections," *Viruses*, vol. 13, no. 8, p. 1488, 2021.
- [34] L. Zhou, W. Chen, H. Yang, J. Liu, and H. Meng, " β Circ_001042 inhibits TGF-1/P38 MAPK signaling axis-mediated epithelial-mesenchymal transition and metastasis in lung adenocarcinoma," *Evidence-based Complementary and Alternative Medicine*, vol. 2022, pp. 1–11, 2022.
- [35] Y. Li, R. Dong, M. Lu et al., "Let-7b-3p inhibits tumor growth and metastasis by targeting the BRF2-mediated MAPK/ERK pathway in human lung adenocarcinoma," *Translational Lung Cancer Research*, vol. 10, no. 4, pp. 1841–1856, 2021.
- [36] J. Cheng, L. Xia, X. Hao et al., "Targeting STT3A produces an anti-tumor effect in lung adenocarcinoma by blocking the MAPK and PI3K/AKT signaling pathway," *Translational Lung Cancer Research*, vol. 11, no. 6, pp. 1089–1107, 2022.
- [37] W. Zhao, L. Liu, X. Li, and S. Xu, "EphA10 drives tumor progression and immune evasion by regulating the MAPK/ERK cascade in lung adenocarcinoma," *International Immunopharmacology*, vol. 110, Article ID 109031, 2022.
- [38] S. Yang, Y. Liu, M. Y. Li et al., "FOXP3 promotes tumor growth and metastasis by activating Wnt/ β -catenin signaling pathway and EMT in non-small cell lung cancer," *Molecular Cancer*, vol. 16, no. 1, p. 124, 2017.
- [39] Y. r. Zhao, J. l. Wang, C. Xu, Y. m. Li, B. Sun, and L. y. Yang, "HEG1 indicates poor prognosis and promotes hepatocellular carcinoma invasion, metastasis, and EMT by activating Wnt/ β -catenin signaling," *Clinical Science*, vol. 133, no. 14, pp. 1645–1662, 2019.
- [40] K. R. Fischer, A. Durrans, S. Lee et al., "Epithelial-to-mesenchymal transition is not required for lung metastasis but contributes to chemoresistance," *Nature*, vol. 527, no. 7579, pp. 472–476, 2015.
- [41] X. Zheng, J. L. Carstens, J. Kim et al., "Epithelial-to-mesenchymal transition is dispensable for metastasis but induces chemoresistance in pancreatic cancer," *Nature*, vol. 527, no. 7579, pp. 525–530, 2015.
- [42] E. Galle, B. Thienpont, S. Cappuyns et al., "DNA methylation-driven EMT is a common mechanism of resistance to various therapeutic agents in cancer," *Clinical Epigenetics*, vol. 12, no. 1, p. 27, 2020.